Journal of Catalysis 279 (2011) 319–327

Contents lists available at ScienceDirect

Journal of Catalysis

journal homepage: www.elsevier.com/locate/jcat

Monoalkylations with alcohols by a cascade reaction on bifunctional solid catalysts: Reaction kinetics and mechanism

Avelino Corma *, Tania Ródenas, María J. Sabater *

Instituto de Tecnología Química, Universidad Politécnica de Valencia–Consejo Superior de Investigaciones Científicas, Avenida Los Naranjos s/n, 46022 Valencia, Spain

ARTICLE INFO

Article history:
Received 23 November 2010
Revised 26 January 2011
Accepted 27 January 2011
Available online 5 March 2011

Keywords:
Bifunctional catalyst
Pd-MgO
Cascade reaction
Hydrogen transfer
Metal nanoparticle
Palladium dihydride
Basic supports

ABSTRACT

A bifunctional catalytic system formed by Pd on MgO catalyzes the cascade process between benzyl alcohol and phenylacetonitrile, diethylmalonate and nitromethane, to give the respective α-monoalkylated products without external supply of hydrogen. The process involves a series of three cascade reactions occurring on different catalytic sites. The alcohol undergoes oxidation to the corresponding aldehyde with the simultaneous formation of a metal hydride; then, the aldehyde reacts with a nucleophile formed "*in situ*" to give an alkene, and finally, the hydrogen from the hydride is transferred to the alkene to give a new C–C bond.

A kinetic study on the α-monoalkylation reaction of benzylacetonitrile with benzyl alcohol reveals that the rate-controlling step for the one-pot reaction sequence is the hydrogen transfer reaction from the surface hydrides to the olefin, and consequently, the global reaction rate is improved when decreasing the size of the Pd metal particle.

1. Introduction

Reactions directing to the formation of C–C bonds are of much interest in synthetic organic chemistry. Among them, the Knoevenagel condensation affords α–β conjugated enones through the nucleophilic addition of active methylene compounds to carbonyl groups, followed by elimination of a molecule of water. For the Knoevenagel reaction, basic catalysts abstract a proton from the activated methylenic group and form the intermediate carbanion (nucleophile) that will react with the carbonyl group to give the olefin. The double bond can be further hydrogenated in a subsequent step to give a saturated compound.

The two reaction steps previously described (Knoevenagel condensation and hydrogenation) can be carried out in one-pot reaction by means of bifunctional metal–base solid catalysts, while working in the presence of hydrogen [1]. However, there is another way to achieve the final hydrogenated product without the need of added hydrogen. This will consist of a one-pot reaction between an alcohol and a molecule having an activated methylenic group in the presence of a bifunctional metal/base solid catalyst.

In this case, the global process involves in the first step an alcohol which is dehydrogenated on the metal function to yield the corresponding aldehyde (or ketone) and a metal hydride. Meanwhile, the basic function of the catalyst will abstract a proton from the activated methylenic group of the second reactant to give the corresponding carbanion. Both the carbanion and the carbonyl compound will react to give an olefinic condensation product and, finally, the metal hydride will transfer the hydrogen to the double bond to give the final saturated product (see Scheme 1).

This sequential process is based on hydrogen transfer from an alcohol that will act as the hydrogen source [2–9] and may also have interesting and useful applications when the intermediate carbonyl compound is unstable, since it will react *in situ*, and its isolation and purification will not be necessary. Moreover, the process described above can be a convenient procedure especially when a chemoselective hydrogenation of the double bond is required [9b,c].

Typical homogeneous catalysts such as Ru-, Rh-, and Ir-based complexes in d^6 and d^8 electronic configuration are recognized to be most efficient catalysts for transfer hydrogenation while, with the exception of Os, other second or third row elements seem to be much less suited for this catalysis [10–12]. In general, transfer hydrogenation with the above metal complexes involves the use of an alcohol that will serve as hydrogen source with the aid of a metal catalyst, and an alkaline agent that is necessary to activate the C–H bond through formation of the alkoxide ion.

Here, we report the formation of C–C bonds starting from an alcohol, by α-monoalkylation reactions using a Pd–MgO bifunctional catalyst. In this case, the metal will perform a dehydrogenation to give the intermediate carbonyl compound and a palladium dihydride [13]. Then, the reaction of the carbonyl with a variety of

* Corresponding authors. Fax: +34 96 3877809.
E-mail address: acorma@itq.upv.es (A. Corma).

0021-9517/$ - see front matter © 2011 Elsevier Inc. All rights reserved.
doi:10.1016/j.jcat.2011.01.029

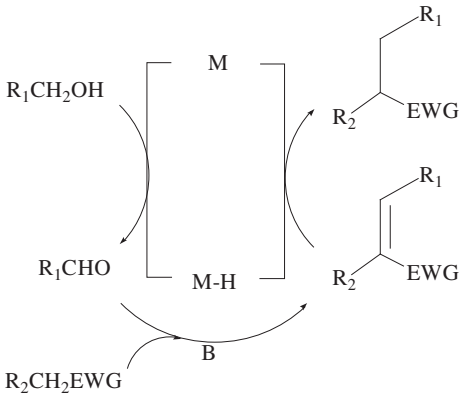

Scheme 1. One-pot α-monoalkylation reaction of methylene compounds with alcohols in the presence of a bifunctional metal–base catalyst (EWG = electron withdrawing group).

methylene compounds with different p*K*s will produce the olefinic condensed products. Finally, the olefins will be hydrogenated to provide the corresponding C–C bond. In this process, which can be considered an extension of the Wittig reaction (well-known method for the conversion of aldehydes into alkenes), an alcohol will serve dually as hydrogen donor and as precursor to the carbonyl electrophile, avoiding the use of homogeneous toxic alkylating agents as well as the formation of dialkylated products.

2. Experimental

Hydroxyapatite (HAP) and hydrotalcite (HT) were prepared following reported procedures [14,15]. A MgO sample with a surface area of 670 m^2/g was purchased from NanoScale Materials. Inorganic salts $Pd(acac)_2$, $NaAuCl_4$, $KAuCN_4$, and $AuPPh_3Cl$ were purchased from Aldrich and $Pt(acac)_2$ was from Acros. The reactants were used without further purification.

2.1. Preparation of catalysts

2.1.1. Preparation of metal (M)–MgO (M = Pd, Pt, Au) bifunctional catalysts

Pd–MgO (0.8 wt.% palladium) was prepared following the procedure reported in [13].

Pt–MgO (1 wt.% metal loading) was obtained by adding 1 g of MgO (670 m^2/g) to 30 ml anhydrous dichloromethane solution containing $Pt(acac)_2$ (24.01 mg, mmol) under stirring for 12 h. After evaporation of the solvent at reduced pressure, the resultant solid was dried overnight at 353 K in vacuum and then calcined in nitrogen flow at 823 K (heating rate: 5 °C/min) for 3.5 h. The sample was activated before reaction by heating the solid at 723 K under air atmosphere for 5 h and then for 5 h under nitrogen. Metal reduction was performed by heating the solid at 523 K in a flow of H_2/N_2 (90/10) for 2 h.

Au–MgO (1 wt.% metal loading) was prepared as follows [16]: 1 g of MgO (670 m^2/g) were added to 30 ml of ethanol solution containing $Au(CH_3)_2(acac)$ (17.963 mg, 0.055 mmol) under stirring for 12 h. The solvent was evaporated at reduced pressure, and the solid was dried overnight at 353 K under vacuum and then calcined in nitrogen flow at 823 K (ramp rate: 5 °C/min) for 3.5 h. The sample was activated before reaction by heating the solid at 723 K under air for 5 h and then for 5 h under nitrogen. Metal reduction was performed by heating the solid at 523 K in a flow of H_2/N_2 (90/10) for 2 h.

Pd–HAP and Pd–HT were prepared according to previous reported procedures [14,15].

2.2. Catalytic tests

2.2.1. α-Monoalkylation of phenylacetonitrile with benzyl alcohol on metal–MgO as catalysts

A mixture of benzyl alcohol (1 mmol), phenylacetonitrile (3 mmol), 0.0998 g of metal–MgO (Pd: 0.0075 mmol; Au: 0.0075 mmol; Pt: 0.0075 mmol), trifluorotoluene (1 ml) and *n*-dodecane (20 μl) as internal standard were placed into an autoclave. The resulting mixtures were vigorously stirred at 180 °C under nitrogen, being monitored by GC.

2.2.2. Catalyzed α-monoalkylation of malonate diester with benzyl alcohol

A mixture of benzyl alcohol (1 mmol), diethylmalonate (3 mmol), 0.0998 g of Pd–MgO (Pd: 0.0075 mmol), trifluorotoluene (1 ml), and *n*-dodecane (20 μl) as internal standard were placed into an autoclave. The resulting mixture was vigorously stirred at 180 °C (or 100 °C) under nitrogen. The reaction was monitored by GC.

2.2.3. Catalyzed α-monoalkylation of nitromethane with benzyl alcohol

Given that oxidation of benzyl alcohol did not occur in the presence of nitromethane (probably due to a strong competitive adsorption of the last molecule on the metal active sites), in this case, the one-pot synthesis was performed in such a way that nitromethane was incorporated when practically all benzyl alcohol was dehydrogenated as follows:

A mixture of benzyl alcohol (1 mmol), 0.0998 g of Pd–MgO (Pd: 0.0075 mmol), trifluorotoluene (1 ml), and *n*-dodecane (20 μl) as internal standard were placed into an autoclave. The resulting mixture was vigorously stirred at 180 °C under nitrogen being monitored by GC. After completing the alcohol transformation to benzaldehyde, nitromethane (3 mmol) was added, and the resulting mixture was vigorously stirred at 180 °C.

3. Results and discussion

The reactivity of Pd on different basic supports such as MgO, Al–Mg hydrotalcite (HT), and hydroxyapatite (HAP) was studied for the α-monoalkylation of phenylacetonitrile with benzyl alcohol as model reaction. 2,3-Diphenylacrylonitrile (**1**) and 2,3-diphenylpropionitrile (**2**), together with small amounts of benzene and toluene, were obtained as reaction products. Better yields of the desired final product (**2**) were obtained with Pd on MgO than on HT or HAP (see entries 1–3, Table 1).

In fact when Pd was supported on Al–Mg hydrotalcite (HT), the resultant catalyst was active but the yield and selectivity to **2** and even **1 + 2** were lower than with MgO. The situation was even worst with HAP, since in this case the basicity was too weak and the catalyst was inactive (see entries 1–3, Table 1). Therefore, on the bases of the results obtained, MgO was selected as the basic component of the bifunctional catalyst.

Fig. 1 shows the evolution with time of the different products obtained when benzyl alcohol and phenylacetonitrile were reacted in the presence of the bifunctional Pd–MgO catalyst.

A priori, formation of the alkene 2,3-diphenylacrylonitrile **1** and 2,3-diphenylpropionitrile **2** can be explained *via* oxidative removal of hydrogen from benzyl alcohol to afford benzaldehyde (not detected by gas chromatography in the presence of the arylnitrile) and a characteristic palladium dihydride intermediate (see Scheme 2) [13,17]. Then, in the presence of the solid base MgO, phenylacetonitrile is activated to give a nucleophile which will rapidly condense with benzaldehyde to give the condensation product **1**, which is hydrogenated by the metal hydride yielding the α-monoalkylated product **2** according to Scheme 2.

Table 1
Results on α-monoalkylation reaction of phenylacetonitrile with benzyl alcohol using diverse bifunctional solid catalysts.[a]

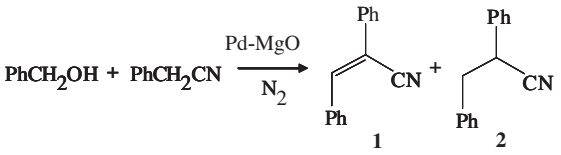

Entry	Catalyst	C[b] (%)	Yield[c] (%)				Time (h)	TON[d]
			1	**2**	PhH	$PhCH_3$		
1	Pd–MgO	99	3	94	2	1	24	459
2	Pd–HT	100	6	79	8	7	21	137
3	Pd–HAP	0	0	0	0	0	0	0
4	Pd–C	43	0	0	11	15	24	78
5	Au–MgO	66	20	0	2	3	48	120
6	Au^{1+}–MgO[e]	60	60	0	Traces	Traces	66	110
7	Au^{1+}–MgO[e,f]	83	74	11	0	Traces	120	120
8	Pt–MgO	95	85	10	0	0	116	207

[a] Reaction conditions: benzyl alcohol (1 mmol), benzylnitrile (3 mmol), *n*-dodecane (0.1 mmol), Pd–MgO (0.0075 mmol Pd), 1 ml trifluorotoluene, $T = 180$ °C.
[b] Conversions were determined by GC on the basis of benzyl alcohol consumption.
[c] Determined by GC.
[d] mmol of substrate converted/mmol catalyst.
[e] $AuPPh_3Cl$ deposited on MgO.
[f] Reaction carried out at 100 °C.

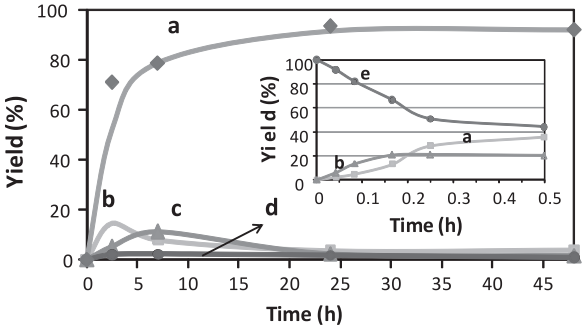

Fig. 1. Plot showing the yields of reaction products *versus* time in the α-monoalkylation reaction of phenylacetonitrile with benzyl alcohol to give the saturated product: (a) 2,3-diphenylpropionitrile **2**, (b) the alkene 2,3-diphenylacrylonitrile **1**, (c) toluene, and d) benzene (entry 1, Table 1). The inset shows the evolution of $PHCH_2OH$ and reaction products at short reaction times: (a) 2,3-diphenylpropionitrile **2**, (b) 2,3-diphenylacrylonitrile **1**, and (e) $PhCH_2OH$.

It is evident from results presented in Fig. 1 that product **1** is a transient product since its yield rises and then falls as expected for a sequential cascade as envisaged. Besides this, there is an induction period in the appearance of **2** as **1** is formed (see inset Fig. 1) that can be observed when the plot is obtained at short reaction times. Nonetheless, benzaldehyde was not detected by gas chromatography in the presence of the arylnitrile, even at short reaction times.

In this case, the formation of very minor amounts of toluene and benzene can be explained by hydrogenolysis of benzyl alcohol and decarbonylation of the intermediate benzaldehyde product, respectively. On the other hand, control reactions showed that either MgO or palladium separately did not catalyze the one-pot reaction albeit, in the absence of base, palladium (supported on carbon) still catalyzes at lower rates the formation of benzaldehyde, producing meanwhile higher yields of toluene and benzene than Pd–MgO (see entry 4, Table 1).

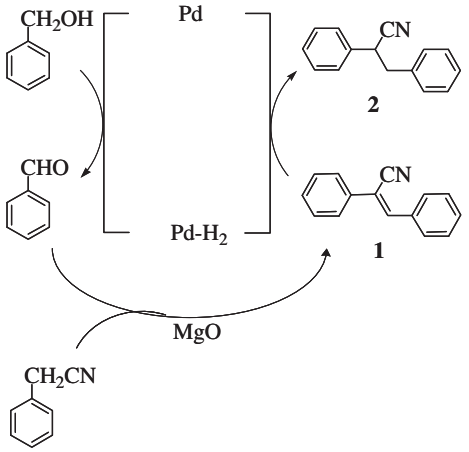

Scheme 2. Schematic representation of α-monoalkylation reaction of phenylacetonitrile with benzyl alcohol catalyzed by Pd–MgO.

The influence of substituents at the aromatic alcohol was also studied, and the results showed that both the position as well as the nature of the substituent had a significant effect on the alkylation reaction (the composition and yield of products are collected in Table 2).

Thus, the introduction of one nitro group at the *para* position of benzyl alcohol led to high yields of monoalkylated product $\mathbf{P_2}$ (entry 2, Table 2) after prolonged reaction time; whereas the same electron withdrawing group at the *meta* position gives lower conversion and yield of $\mathbf{P_2}$ (entry 8, Table 2). With electron donor groups at the *para* position (amino and methoxy groups), similar high yields of saturated product $\mathbf{P_2}$ could be obtained in both cases (entries 3, 4 in Table 2).

The observation that *p*-substituents having electron withdrawing or electron donating character both reduce the apparent reactivity of benzyl alcohol is not evident. Probably, this should be attributed to a preferential adsorption of these groups over the hydroxy group, a fact that may slow down the transformation of the alcohol into the corresponding aldehyde.

The introduction of two fluorine atoms at the *ortho* position resulted in a net electron withdrawing effect and an increase of the steric hindrance for α-monoalkylation. This fact accounted for the longer reaction times required to achieve from low to moderate yields of $\mathbf{P_2}$ (see entries 5 and 7 in Table 2).

Besides phenylacetonitrile, other methylene compounds such as nitromethane and diethyl malonate were also studied by applying the same methodology. In this case, the proton abstraction at the α-C–H position of the above molecules generates two different nucleophiles that immediately add to the aldehyde formed by alcohol dehydrogenation, giving the unsaturated compounds **3** and **5**, respectively (see Scheme 3 and entries 3–5 in Table 3).

Subsequent reduction of these two products by the intermediate palladium hydride complex formed during the dehydrogenation step leads to formation of the corresponding hydrogenated products **4** and **6** (see Scheme 3 and entries 3–5 in Table 3).

It is interesting to notice that the reaction with nitromethane was the slowest one, partly because this compound was not incorporated during the initial stages of reaction, but after benzyl alcohol was completely transformed into benzaldehyde. Effectively, given that oxidation of benzyl alcohol did not occur in the presence of nitromethane (probably due to a strong competitive adsorption of the last molecule on the metal active sites), in this case, the one-pot synthesis was performed in such a way that nitromethane was incorporated when practically all benzyl

Table 2
α-Monoalkylation reaction of phenylacetonitrile with benzyl alcohol derivatives over bifunctional Pd–MgO catalyst.[a]

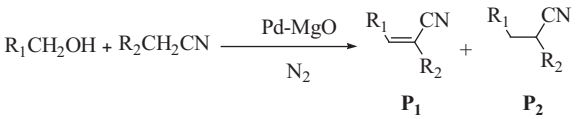

Entry	Substrate	Alcohol	Time (h)	C[b] (%)	Yield[c] (%)		TON[d]
					P_1	P_2	
1	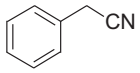	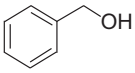	7	99	3	94	459
2	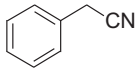	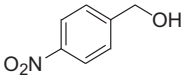	16	100	11	86	123
3	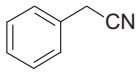	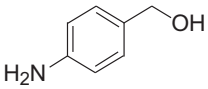	16	84	13	73	119
4	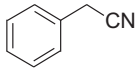	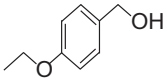	28	93	12	76	107
5	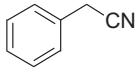	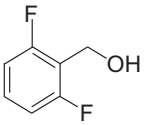	32	70	12	54	82
6	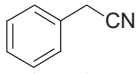	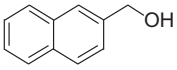	24	73	58	15	98
7	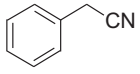	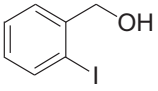	24	65	10	10	77
8	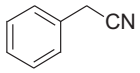	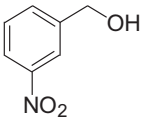	24	17	4	9	22

[a] Reaction conditions: alcohol (1 mmol), phenylacetonitrile (3 mmol), *n*-dodecane (0.1 mmol), Pd–MgO (0.0075 mmol Pd), 1 ml trifluorotoluene, $T = 180$ °C under N_2.
[b] Conversions were determined by GC on the basis of alcohol consumption.
[c] Determined by GC.
[d] mmol of substrate converted/mmol catalyst.

alcohol was dehydrogenated (Fig. 2 shows the evolution of conversion and yields of final hydrogenated products with time).

It is also worth mentioning that the conversion of benzyl alcohol was much more rapid in the case of diethyl malonate; however, contrarily to our initial expectations, the respective hydrogenated product (product **6**) evolved much more rapidly in the case the phenylacetonitrile (product **2**) (see Fig. 2). The reason relies in the fact that diethyl malonate was immediately transformed into a mixed diester before being converted into the desired monoalkylated product during the early stages of the reaction.

Effectively, in the case of β-diester, the monotransesterification reaction efficiently competed with α-monobenzylation to give a mixed diester derived from malonic acid (benzyl ethyl malonate), especially at low conversions and low temperatures. In accordance with this, the mixed diester was isolated as main product when the reaction was carried out at 100 °C (see entry 5, Table 3). At higher temperatures (180 °C), the mixed diester (in equilibrium with diethyl malonate) was detected only at low conversions, since α-monoalkylation shifted progressively the equilibrium toward the alkylated product **6**.

Since the slowest step in a multistep reaction will determine the rate of the entire sequence, we have attempted to identify the rate-controlling step of this complex mechanism, since this should give information on the function of the catalyst that should be improved. The rate-controlling step was determined by means of a kinetic study of the α-monoalkylation of phenylacetonitrile with benzyl alcohol.

3.1. Optimization of the bifunctional catalyst

3.1.1. Elucidation of the rate-controlling step in the α-monoalkylation of phenylacetonitrile with benzyl alcohol

The three elementary steps of the overall reaction are given in Eqs. (1)–(3), where k_a, k_b, and k_c are the corresponding rate kinetic constants:

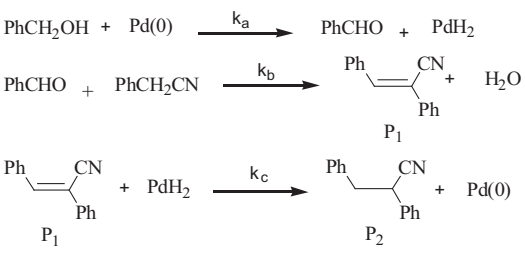

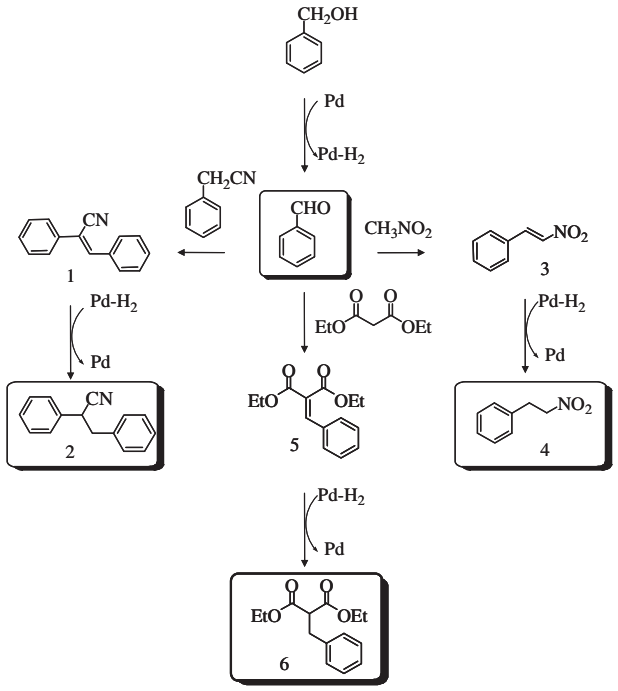

Scheme 3. Schematic representation of the α-monoalkylation reaction of phenylacetonitrile, diethylmalonate, and nitromethane with benzyl alcohol over Pd–MgO.

In principle, three kinetic rate expressions can be derived by considering that the dehydrogenation of benzyl alcohol to give benzaldehyde and metal hydride (Eq. (1)), or the condensation reaction (Eq. (2)), or the hydrogenation (Eq. (3)) is the overall rate-controlling step.

Nonetheless, *a priori*, the possibility that the first step, which is the dehydrogenation of the alcohol, would be controlling was rejected based on the observation that the initial reaction rate r_0 is first order with respect to alcohol ([$PhCH_2OH$]) and first order with respect to phenylacetonitrile ([$PhCH_2CN$]) (see Fig. 3 and Supplementary Material).

In accordance with these results, it may be that either the condensation reaction or the hydrogen transfer reaction (Eqs. (2) and (3)) would be the reaction-controlling step during the one-pot reaction. Thus, we carried out a series of additional experiments, in which the dehydrogenation of the alcohol (to give benzaldehyde and palladium dihydride) was studied in two different experiments separately

In this case, an initial amount of benzyl alcohol and the catalyst (Pd–MgO) was incorporated into two separate equal reactors, leading to formation of PhCHO and Pd–H_2 in both cases. At this point, equimolar amounts of $PhCH_2CN$ and the alkene **1** (P_1) were incorporated into the first and second reactors, respectively, and the initial reaction rates (r_0) for the condensation and hydrogenation reactions were calculated (see Fig. 4).

Under the above experimental conditions, it was observed that the hydrogenation of the alkene P_1 by the surface hydrides was slower than the condensation reaction with the activated

Table 3
α-Monoalkylation reaction of phenylacetonitrile, diethyl malonate, and nitromethane with benzyl alcohol over bifunctional Pd–MgO as catalyst.[a]

Entry	Substrate	Time (h)	C[b] (%)	Yield[c] (%)							TON[d]
				1	**2**	**3**	**4**	**6**	PhH	$PhCH_3$	
1	$PhCH_2CN$	7	99	3	94				1	Traces	459
2[e]	$PhCH_2CN$	24	43	0	0				11	15	78
3	CH_3NO_2	40	84			6	78		0	0	66
4	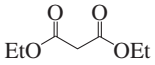	2	100					99	0	0	126
5[f,g]	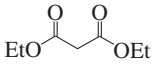		76					7	1.5	1.5	94

[a] Reaction conditions: benzyl alcohol (1 mmol), substrate (3 mmol), *n*-dodecane (0.1 mmol), Pd–MgO (0.075 mmol Pd), 1 ml trifluorotoluene, $T = 180$ °C under N_2.
[b] Conversions were determined by GC on the basis of benzyl alcohol consumption.
[c] Determined by GC.
[d] mmol of substrate converted/mmol catalyst.
[e] Pd/C (Norit).
[f] Reaction carried out at 100 °C.
[g] The mixed ester benzyl ethyl malonate was obtained as major product (69% yield).

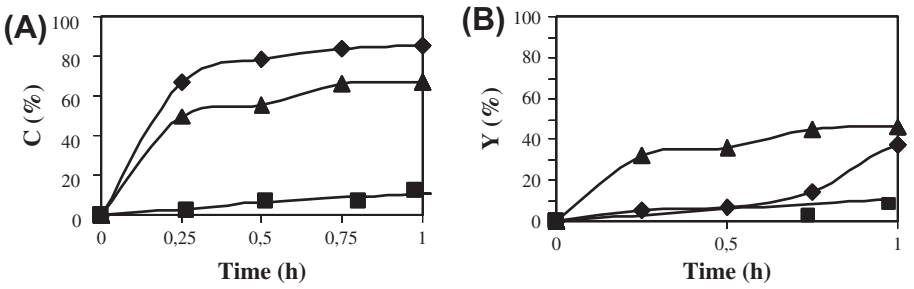

Fig. 2. Comparative plots showing the (A) conversion of benzyl alcohol against time in the reactions with diethyl malonate (♦), phenylacetonitrile (▲), and nitromethane (■), and (B) yields of compounds **2**, **4**, and **6** derived from reactions of benzyl alcohol with diethyl malonate (♦), phenylacetonitrile (▲), and nitromethane, respectively (■) *versus* time in the presence of Pd–MgO as catalyst (0.8%; 0.0075 mmol Pd).

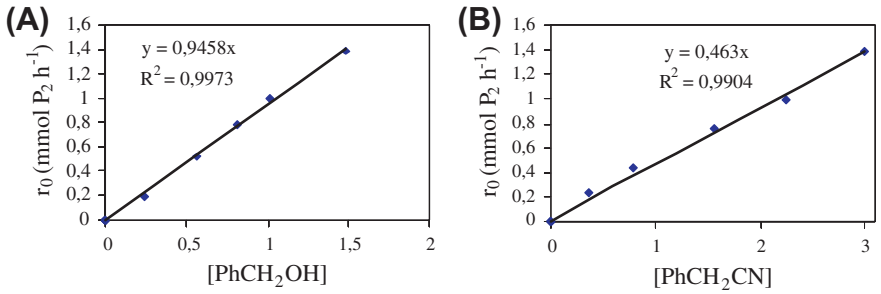

Fig. 3. Graphic representations obtained when plotting (A) r_0 *versus* [$PhCH_2OH$] and (B) r_0 *versus* [$PhCH_2CN$].

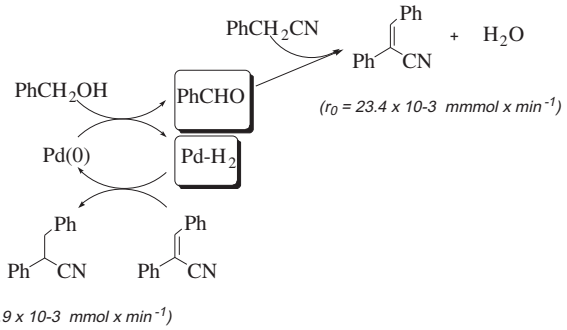

Fig. 4. Schematic representation of kinetic experiments to calculate the condensation and hydrogenation reaction rates.

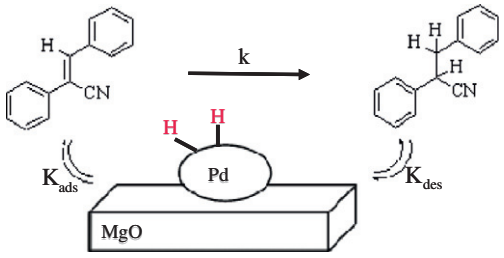

Fig. 5. Graphic representation of the hydrogenation of P_1 at the surface of Pd–MgO.

methylenic compound. Even though the situation is not the same from the global reaction point of view, the result supports the conclusion that the catalytic function that will determine the rate of the overall process corresponds to the metal hydride function on the metal surface (Pd–H) and not the basic function of the catalyst, i.e., MgO. This is an important conclusion since it indicates which one of the components of the bifunctional catalyst has to be improved.

Once it was established that the step corresponding to the transfer of the metal hydride to the olefin was the controlling step, we have still to find out if the adsorption of reactants, desorption of products or the surface reaction was the final controlling step during the hydrogenation process. Then, in order to address this question, a new kinetic study was undertaken.

3.2. Determination of adsorption (K_{ads}), desorption (K_{des}), and reactivity constants (k_r) during the hydrogenation transfer step from Pd–H to P_1 [18]

It was assumed in this study that the surface of the solid was uniform, and a number of adsorption sites were available to the reactants. On these sites, the condensation product P_1 would adsorb on active sites following a Langmuir type isotherm, with K_{ads} as adsorption constant (Fig. 5).

Then, the adsorbed P_1 molecules will react with the metal hydrides Pd–H (k), previously formed at the metal surface to give the hydrogenated product P_2, which would be desorbed at the end (K_{des}) (see Fig. 5).

On these premises, three possible rate expressions or models derived from the *Langmuir–Hinshelwood* methodology were postulated assuming that either adsorption, desorption, or the surface reaction were the controlling step in the hydrogenation process [18]. In this case, the concentrations of PhCHO, $PhCH_2CN$, and P_2 were also included in the equations since, even though they are not involved in the hydrogen transfer, they can compete with P_1 for adsorbing on the metal active sites.

Model 1

The adsorption of P_1 is the rate-controlling step:

$$r_0 = \frac{k[P_1]}{1 + K_{des}(P_2)[P_2] + K_i[I]}$$

Model 2

The hydrogenation reaction of P_1 is the rate-controlling step:

$$r_0 = \frac{k[P_1]}{1 + K_{ads}(P_1)[P_1] + K_{des}(P_2)[P_2] + K_i[I]}$$

Model 3

Desorption of P_2 is the rate-controlling step.

$$r_0 = \frac{k[P_1]}{1 + K_{ads}(P_1)[P_1] + K_i[I]}$$

where k is the kinetic rate constant, K_{ads} is the adsorption equilibrium constant, K_{des} is the desorption equilibrium constant, and K_i is the adsorption equilibrium constant for other molecules.

A set of 33 kinetic experiments was designed, and the numerical results were fitted by least squares using the tool Solver on the Excel 3.0 program (see Table 1S in Supplementary Material) [18]. The correlation coefficient R^2 (or cross-correlation coefficient) was used as criterium to discern among the best least squares fitting for the three possible models (see Tables 2S–4S in Supplementary Material), and Table 4 collects the calculated parameters.

According to these calculations, the model that best fits the experimental data corresponds to the surface reaction (model 2). So again this fact corroborates that the catalytic function that will determine the rate of overall process with the Pd–MgO catalyst is indeed the metal hydride function on the surface (Pd–H) of the catalyst and no the basic function of the catalyst, i.e., MgO.

At this point, and in order to increase the rate of hydrogenation, we have on one hand changed the hydrogenation function (Pd, Pt, and Au), and on the other hand, the crystallite size of the best operating metal has also been varied.

Table 4
Constant values obtained for the different models in the presence of inert molecules (P_2, PhCHO and $PhCH_2CN$) based on least squares adjustment using the tool Solver on the Excel 3.0 program.

Model	k	$K_{ads}(P_1)$	$K_{des}(P_2)$	$K_{ads}(PhCH_2CN)$	$K_{ads}(PhCHO)$	$\sum[r_0(exp) - r_0(mod)]^2$	R^2
1	0.803	0.001	0.592	0.083	0.058	0.024	0.96
2	0.91	0.23	0.71	0.10	0.09	0.020	0.96
2[a]	0.89	0.22	0.63	0.14	0.05	0.006	0.99
3	0.0867	0.198	0.001	0.0093	0.0093	0.029	0.95

[a] Constant values obtained with $[PhCH_2CN] = 3$ mmol/ml.

3.3. Influence of the nature of the metal

Au–MgO was found to be inactive for catalyzing the global reaction, though benzyl alcohol afforded reasonable yields of benzaldehyde when a gold (I) salt was deposited on MgO in two additional experiments either at 100 °C or at 180 °C (see entries 5–7 in Table 1).

With platinum supported onto MgO, the alcohol was almost completely transformed into benzaldehyde that condensates to give **1**, but the yields of **2** are much lower than those obtained with palladium (compare entries 1 and 8 in Table 1). The clear superiority of palladium over gold and platinum for catalyzing this reaction can be explained by taking into account that the stability of gold and platinum hydrides are either too low or too high, respectively, and consequently, they are less reactive than palladium hydrides [19–22].

This explanation is in line with the previous observation that the controlling step of the reaction is the hydrogenation of the double bond through hydrogen transfer from the metal hydride, and consequently, the surface hydride concentration and its ability to release the hydrogen will determine the activity and selectivity of the catalyst.

If Pd was the metal of choice, we could still improve its reactivity by optimizing the crystallite metal size.

3.4. Influence of Pd crystallite size

The concentration of surface hydrides on Pd could be varied by changing the metal crystallite size. Then, different Pd–MgO catalysts were prepared with average Pd metal particle size ranging from 2.2 to 5.3 nm, and the number of Pd surface atoms in each sample was calculated taking into account the total metal content and crystal size distribution, following the calculation procedure given in [23a–d].

TOFs were calculated by dividing the initial reaction rate by the number of surface metal atoms, and the results were plotted *versus* the average particle size for the different catalysts (see Fig. 6).

As can be deduced from Fig. 6, it is evident that TOF increases when decreasing the Pd crystallite size, especially for the hydride transfer reaction (see curve a) in Fig. 6), while remains practically constant for those reactions giving the subproducts toluene and benzene. Then, it appears that the reaction considered here is a structure sensitive reaction [23e] that requires highly dispersed Pd on MgO.

3.5. Reaction mechanism

In order to better define the metal active species and their mechanistic cycle for the overall process, we have followed the reaction by DR–UV visible. The results given in Fig. 7 show that a freshly prepared Pd–MgO catalyst gives a spectrum with a broad and structureless band at 300 nm that has been assigned to Pd(0) [24]. On the other hand, the formation of different palladium species during reaction was detected through the analysis of the DR–UV–vis spectra of the solid at different reaction times (Fig. 7).

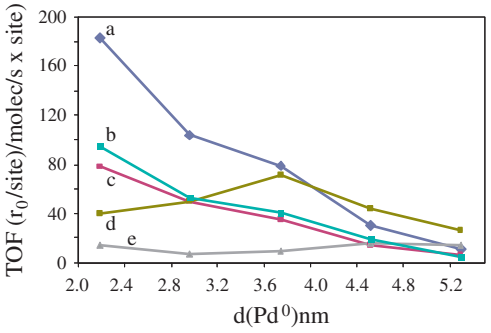

Fig. 6. Plots showing the initial reaction rates (r_0) per surface atom as a function of metal particle size for: (a) the hydrogenation transfer reaction to afford **2**; (b) dehydrogenation of benzyl alcohol to afford benzaldehyde; (c) condensation reaction to give **1**; (d) hydrogenolysis reaction to give toluene, and (e) decarbonylation reaction to afford benzene.

The spectrum of the catalyst recovered after completing the benzylic alcohol transformation to benzaldehyde (in the absence of the arylnitrile) was very similar to that of $Pd(acac)_2$ (Fig. 7), hence suggesting an initial oxidative addition process from Pd^0 to afford the intermediate Pd^{2+} dihydride with simultaneous formation of benzaldehyde.

After adding phenylacetonitrile, formation of the Knoevenagel condensation product **1** occurs being smoothly converted into the target product **2**. At this point, the DR–UV–vis spectrum of the solid was again recorded, showing that the initial broad band at 315 nm was again restored. These spectral changes confirm that the catalysis by palladium involves the transition between the Pd^0 and Pd^{2+} oxidation states [13].

The formation of palladium dihydride species over Pd–MgO has been indirectly confirmed by the identification of the corresponding deuterium labeled species using NMR spectroscopy [13]. This, together with the fact that the controlling step of the reaction

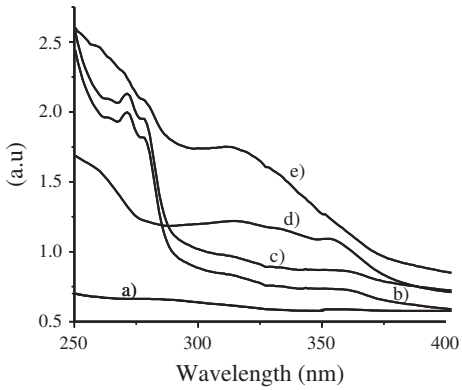

Fig. 7. DR–UV–vis spectra of (a) MgO, (b) Pd(acac)2, (c) Pd–MgO recovered after completing the benzyl alcohol transformation to benzaldehyde (before the arylnitrile addition), (d) Pd–MgO recovered at the end of reaction (after the arylnitrile addition), and (e) fresh prepared Pd–MgO sample.

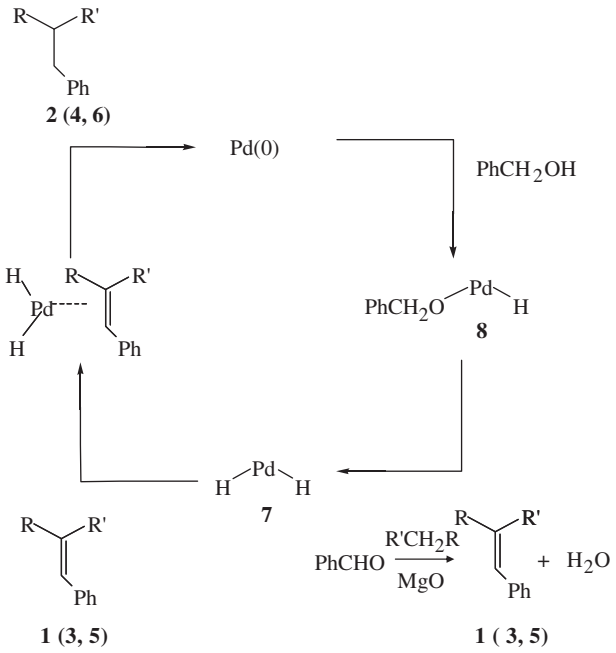

Scheme 4. Proposed reaction mechanism for the α-monoalkylation of phenylacetonitrile, diethyl malonate, and nitromethane with benzyl alcohol catalyzed by Pd–MgO under inert atmosphere.

corresponds to the transfer of hydride to the alkene **1**, led us to propose the following tentative reaction mechanism for the monoalkylation of phenylacetonitrile, and by extension to nitromethane and malonic ester, on Pd–MgO as catalysts (see Scheme 4).

In this mechanism, palladium dihydride species Pd–H_2 (**7**) are formed upon direct interaction with the alcohol (and/or through formation of a palladium alkoxylate intermediate **8**). The dihydride metal species **7** react with the resulting unsaturated compounds **1**, **3**, and **5** formed after condensation reaction of benzaldehyde with the respective nucleophile (formed *in situ* on the basic sites of MgO) to give the hydrogenated compounds **2**, **4**, and **6**.

3.6. Catalyst recycle

Reusability experiments have been carried out after separation of the Pd–MgO catalyst by filtration, followed by an exhaustive washing with trifluorotoluene and calcination. The resultant sample was used in a second cycle and showed a similar activity in its reuse. It was found from ICP-AES that metal leaching from the MgO surface could not be detected. Moreover, when analyzing by TEM the solid after recovering, it was observed that the size of Pd nanoparticles was still optimal, while the XRD spectrum of the MgO before calcination experienced noticeable changes. XRD revealed that during the process, the support undergoes a phase transformation to $Mg(OH)_2$ (see Fig. S1 in Supplementary Material) that is transformed back into MgO upon calcination.

4. Conclusions

Pd–MgO catalyzes selectively the sequential oxidation of benzyl alcohol to benzaldehyde and the generation of carbon nucleophiles by activation of the α-C–H bond adjacent to different substrates, i.e., α-arylnitrile, β-diester, and nitro compound derivatives. The resulting nucleophiles will rapidly condense to afford a double bond that will be hydrogenated at the end.

A kinetic study for the α-monoalkylation reaction of benzylacetonitrile with benzyl alcohol shows that the rate-controlling step for the one-pot reaction sequence is the hydrogenation of the olefin by the surface metal hydrides being highly dispersed Pd a very adequate metal function.

A molecular mechanistic cycle has been presented which was supported by kinetic, isotopic, and DR–UV–vis spectroscopic studies.

The utility of the present catalytic system has to do with the avoidance of toxic classic alkylating agents and the concurrent formation of undesirable waste salts as well as the formation of dialkylated byproducts as side reaction.

Acknowledgments

Financial support by Ministerio de Educación y Ciencia e Innovación (Project MIYCIN, CSD2009-00050; *PROGRAMA CONSOLIDER.INGENIO* 2009) and Generalidad Valenciana (GV PROMETEO/2008/130) is gratefully acknowledged. T.R. thanks to Consejo Superior de Investigaciones Científicas for an I3-P fellowships.

Appendix A. Supplementary data

Supplementary data associated with this article can be found, in the online version, at doi:10.1016/j.jcat.2011.01.029.

References

[1] (a) B. Breit, S.K. Zahn, Angew. Chem. Int. Ed. 40 (10) (2001) 1910;
(b) D. Tichit, B. Coq, Cat. Chem. 7 (6) (2003) 206;
(c) D.B. Ramachary, M. Kishor, J. Org. Chem. 72 (14) (2007) 5056;
(d) S. Iborra, A. Corma, J. Catal. 2 (2009) 500. 2;
(e) M.J. Climent, A. Corma, S. Iborra, Chem. Sus. Chem. 2 (2009) 500. 2.
[2] R.L. Augustine, Adv. Catal. 25 (1976) 56.
[3] P. Rylander, Catalytic Hydrogenation in Organic Synthesis, Academic Press, New York, 1979.
[4] M. Hudlicky, Reductions in Organic Chemistry, Wiley, New York, 1984.
[5] S. Siegel, in: B.M. Trost, I. Fleming (Eds.), Comprehensive Organic Synthesis, vol. 8, Pergamon Press, Oxford, 1991 (Chapter 3.1).
[6] H. Takaya, R. Noyori, in: B.M. Trost, I. Fleming (Eds.), Comprehensive Organic Synthesis, vol. 8, Pergamon Press, Oxford, 1991 (Chapter 3.2).
[7] E. Keinan, N. Greenspoon, in: B.M. Trost, I. Fleming (Eds.), Comprehensive Organic Synthesis, vol. 8, Pergamon Press, Oxford, 1991 (Chapter 3.5).
[8] A.J. Birch, D.H. Williamson, Org. React. 24 (1976) 1.
[9] (a) M. Hudlicky, Reductions in Organic Chemistry, second ed., American Chemical Society, Washington, DC, 1996 (Chapter 13);
(b) N. Uematsu, A. Fujii, S. Hashiguchi, T. Ikariya, R. Noyori, J. Am. Chem. Soc. 118 (1996) 4916;
(c) K. Fujita, C. Kitatsuji, S. Furukawa, R. Yamaguchi, Tetrahedron Lett. 45 (2004) 3215.
[10] S. Gladiali, E. Alberico, Transferhydrogenations, in: M. Beller, C. Bolm (Eds.), Transition Metals for Organic Synthesis, vol. 2, second ed., Wiley-VCH Verlag GmbH & Co. KGaA, Weinheim, Germany, 2004.
[11] C. Löfberg, R. Grigg, M.A. Whittaker, A. Keep, A. Derrick, J. Org. Chem. 712 (2006) 8023.
[12] K. Motokura, D. Nishimura, K. Mori, T. Mizugaki, K. Ebitani, K. Kaneda, J. Am. Chem. Soc. 126 (2004) 5662.
[13] A. Corma, M.J. Sabater, T. Ródenas, Chem. Eur. J. 16 (2010) 254.
[14] (a) Kohsuke Mori, Takayoshi Hara, Tomoo Mizugaki, Kohki Ebitani, Kiyotomi Kaneda, J. Am. Chem. Soc. 126 (2004) 10657;
(b) A. Abad, C. Almela, A. Corma, H. García, Tetrahedron 62 (2006) 6666;
(c) C. Elliot, Structure and Chemistry of the Apatites and Other Calcium Orthophosphates, Elsevier, New York, 1994;
(d) C. Elliot, J. Chem. Soc. Faraday Trans. 92 (1996) 293.
[15] F. Cavani, F. Trifirò, A. Vaccari, Catal. Today 11 (1991) 173.
[16] (a) M.J. Climent, A. Corma, S. Iborra, M. Mifsud, J. Catal. 247 (2007) 223;
(b) Y. Hao, M. Mihaylov, E. Ivanova, K. Hadjiivanov, H. Knözinger, B.C. Gates, J. Catal. 261 (2009) 137.
[17] (a) J.S.M. Samec, J.-E. Bäckvall, P.G. Andersson, P. Brandt, Chem. Soc. Rev. 35 (2006) 237;
(b) O. Pamies, J.-E. Bäckvall, Chem. Eur. J. 7 (2001) 5052;
(c) Y.R.S. Laxmi, J.-E. Bäckvall, Chem. Commun. (2000) 611.
[18] (a) J.M. Smith, Chemical Engineering Kinetics, McGraw-Hill International, 1984;
(b) F. Pukelsheim, J.L. Rosengerger, Experimental designs for model discrimination, J. Am. Stat. Assoc. 88 (1993) 642;
(c) P. Zamostny, Z. Belohlav, Identification of kinetic models of heterogeneously catalyzed reactions, Appl. Catal. A 225 (2002) 291.
[19] (a) J.-P. Deng, W.-C. Shih, C.-Y. Mou, Chem. Phys. Chem. 6 (2005) 2021;
(b) A.S.K. Hashmi, R. Salathe, T.M. Frost, L. Schwarz, J.-H. Choi, Appl. Catal. A 291 (2005) 238.

[20] (a) M.C. Gimeno, A. Laguna, in: D.E. Fenton (Ed.), Comprehensive Coordination Chemistry II, vol. 6, Elsevier, Amsterdam, p. 911 (Chapter 6.7).;
(b) R.J. Puddephatt, in: G. Wilkinson (Ed.), Comprehensive Coordination Chemistry, vol. 5, Elsevier, Amsterdam, p. 861 (Chapter 55).
[21] G.N. Khairallah, R.A.J. O'Hair, M.I. Bruced, Dalton Trans. (2006) 3699.
[22] (a) E. Suchanek, N. Lange, G. Auffermann, W. Bronger, H.D. Lutz, J. Raman Spectrosc. 30 (1999) 981;
(b) Raman studies which are a valuable tool in elucidating the relative strength of metal–hydrogen bonds in transition metal hydrido complexes confirms that MH stretching modes display much stronger bonds in the case of 5d metal atoms than the 3d and 4d metal atoms.;
(c) P. Pyykko, Chem. Rev. 88 (1988) 563.
[23] (a) N. Mahata, V. Vishwanathan, J. Catal. 196 (2000) 262;
(b) S. Domínguez-Domínguez, A. Berenguer-Murcia, A. Linares-Solano, D. Cazorla-Amorós, J.Catal. 257 (2008) 87;
(c) R. Van Hardeveld, F. Hartog, Surf. Sci. 15 (1969) 189;
(d) R.E. Benfield, J. Chem. Soc. Faraday Trans. 88 (1992) 1107;
(e) M. Boudart, Chem. Rev. 95 (3) (1995) 661.
[24] (a) A. Corma, H. García, A. Leyva, J. Mol. Catal. A: Chem. 230 (2005) 97;
(b) A. Corma, H. García, A. Leyva, J. Catal. 225 (2004) 350.